drones

MDPI

Article

Online Autonomous Motion Control of Communication-Relay UAV with Channel Prediction in Dynamic Urban Environments

Cancan Tao * and Bowen Liu

School of Automation Science and Electrical Engineering, Beihang University, Beijing 100191, China; liub0020@e.ntu.edu.sg

* Correspondence: taocancan@buaa.edu.cn

Abstract: In order to improve the network performance of multi-unmanned ground vehicle (UGV) systems in urban environments, this article proposes a novel online autonomous motion-control method for the relay UAV. The problem is solved by jointly considering unknown RF channel parameters, unknown multi-agent mobility, the impact of the environments on channel characteristics, and the unavailable angle-of-arrival (AoA) information of the received signal, making the solution of the problem more practical and comprehensive. The method mainly consists of two parts: wireless channel parameter estimation and optimal relay position search. Considering that in practical applications, the radio frequency (RF) channel parameters in complex urban environments are difficult to obtain in advance and are constantly changing, an estimation algorithm based on Gaussian process learning is proposed for online evaluation of the wireless channel parameters near the current position of the UAV; for the optimal relay position search problem, in order to improve the real-time performance of the method, a line search algorithm and a general gradient-based algorithm are proposed, which are used for point-to-point communication and multi-node communication scenarios, respectively, reducing the two-dimensional search to a one-dimensional search, and the stability proof and convergence conditions of the algorithm are given. Comparative experiments and simulation results under different scenarios show that the proposed motion-control method can drive the UAV to reach or track the optimal relay position and improve the network performance, while demonstrating that it is beneficial to consider the impact of the environments on the channel characteristics.

Keywords: unmanned aerial vehicle; communication relay; channel estimation; motion control; Gaussian process; gradient method; wireless networks

Citation: Tao, C.; Liu, B. Online Autonomous Motion Control of Communication-Relay UAV with Channel Prediction in Dynamic Urban Environments. *Drones* **2024**, *8*, 771. https://doi.org/10.3390/drones8120771

Academic Editors: Carlos Tavares Calafate, Higinio González Jorge, Fernando Veiga López, Enrique Aldao Pensado and Gabriel Fontenla-Carrera

Received: 25 October 2024
Revised: 16 December 2024
Accepted: 17 December 2024
Published: 19 December 2024

1. Introduction

Compared with a single agent, a multi-agent system can collaboratively complete tasks more efficiently and economically. In the past few decades, systems composed of multi-agents have shown great advantages in both military and civilian fields by collaborating to learn and adapt in harsh and unknown environments to achieve common goals [1]. Communication and information exchange play a critical role in the success of tasks in multi-agent systems; however, the increase in distance makes it difficult for the agent in the system to meet these requirements [2].

Using communication relays between intelligent nodes is a possible solution [3], and UAVs are particularly suitable for this task. Traditional base stations are not flexible enough and have high costs. Due to their small size, low cost, and flexibility, UAVs are showing a diversified development trend in the military field and are gradually playing a more important role in the field of communication relay [4]. Compared with ground and satellite relays, UAVs have better relay performance [5]. In addition, this kind of instant communication relay without human intervention can be easily deployed; for example, it can be quickly deployed in the event of communication link failures, and

it has the advantages of high adaptability and strong survivability, especially in harsh environments [6].

Dixon et al. [7] proposed an adaptive planning framework based on extremum-seeking control to drive a UAV to a position that improves the chain capacity in point-to-point communication. Its advantage is that even in the presence of unknown interference sources, the performance output can be utilized to drive the UAV to the optimal relay point searched in real time, and only the node position and the sampled objective function value need to be obtained. Yaliniz et al. [8] focused on solving the deployment problem of using UAVs as aerial relays to assist ground cellular networks. They derived a closed-form solution based on a mixed-integer nonlinear optimization method and also considered the effect of UAV altitude on relay-deployment performance when maximizing network performance. Choi et al. [9] used energy efficiency as a metric and maximized the relay energy efficiency through optimizing the UAV speed and load, thereby improving the communication efficiency of a single relay UAV connecting two fixed ground units. However, in these works, user nodes are assumed to be stationary.

Others focus on using the UAV to enhance communication among mobile nodes. Huang et al. [10] aimed to use UAVs to assist in IoT data collection, introduced aerial collaborative relay transmission between UAVs, and proposed an AOI-sensitive data-collection scheme to iteratively optimize the UAV flight paths, solving the problem that UAVs in edge areas need to fly long distances to send data to the base station. Kim et al. [11] proposed a relay UAV motion-planning method based on NMPC and a minimum spanning tree in a dynamic environment, aiming to enhance the communication among a fleet of naval ships. Based on Kim's work, Lun et al. [12] focused on using solar-powered UAVs as communication relays to assist communication among a fleet of ships. Taking both communication connectivity and energy absorption into consideration, they provided the optimal relay path of the SUV, which has a longer flight endurance. Jian et al. [13] proposed an optimization method for simultaneously designing beamforming (BF) and flight trajectory to improve the communication performance between moving users and ground stations using the UAV. The BF weight vectors and the heading angle of the UAV were solved, and experimental results showed that the flight trajectory generated by the proposed method was close to optimal. Although these works have been proven to be suitable for supporting communication for moving users, they all adopted relatively simple communication channel models. These models are actually over-simplified, which will lead to a decrease in the final communication performance [14] and are difficult to use in complex environments. Therefore, it is necessary to use more realistic wireless communication models in research.

Chamseddine et al. [15] proposed a control law to control the UAV to fly to the optimal point without knowing the user's location. This method requires simultaneous measurement of the power and AoA for each ground user. However, due to the diversity of ground users and the different communication devices they carry, it is quite difficult to obtain these two types of information for each ground user at the same time [16]. Hyondong et al. [17] proposed a communication-aware motion-planning method based on NMPC (Nonlinear Model Predictive Control). The main idea is to maintain the LOS (Line of Sight) channel between the relay and the user according to the communication feasible area that changes dynamically with the user's movement. Yin et al. [18] addressed the problem of using relays to enhance data transmission between remote mission UAVs and the ground base station. Considering the signal-propagation characteristics, antenna characteristics, and environmental characteristics, they proposed an algorithm that combines mixed-integer nonlinear programming and the consensus-based bundle algorithm to solve the problem, achieving maximum communication performance with a minimum number of relays. Although these research works consider moving nodes and more realistic channel models, the RF channel parameters of the task environment are still assumed known. However, it is quite difficult to acquire the RF channel parameters of the entire task environment in

advance, as wireless channel parameters are variable and influenced by various factors such as user type, obstacles, weather, etc.

Wu et al. [19] proposed a least squares-based algorithm to predict the RF channel parameters of the task environment for online autonomous motion control of relay UAVs in unknown channels, achieving the goal of enhancing the communication quality of the airborne multi-agent system using a single UAV. However, this work assumes that the aerial environment in which the agent operates is single and simple, without obstacles or other interference, making it difficult to directly apply to other relay tasks with slightly more complex environments. Kim et al. [20] proposed a novel relay UAV-positioning method with channel prediction to enhance the communication quality of multiple moving users in uncertain environments and sought the optimal relay position through an optimization method based on Social Learning Particle Swarm Optimization (SL-PSO). However, this method is time-consuming. Ladosz et al. [21] considered that wireless channel parameters may change during the task and suggested a neural network-based algorithm to predict the channel parameters, and they planned the relay flight trajectory through a rolling-horizon optimization algorithm. However, this channel-prediction method requires the simultaneous collection of communication-strength data and angle-of-arrival information of the signal.

In addition, when conducting online autonomous motion control of the relay UAV, if the impact of different environment types and environmental changes on the relay communication performance can be taken into account, the communication quality of the entire network can be further improved.

In this context, this article proposes a novel relay UAV motion-control method to drive a single UAV to the desired position while considering the UAV's kinematic constraints to achieve optimal communication network performance. The main contributions are as follows: (1) Jointly consider unknown multi-user mobility, unknown RF channel parameters, environmental complexity, and unavailable angle-of-arrival information of the received signals. In addition, when optimizing network performance, the impact of environmental changes on channel characteristics and relay performance is considered. (2) An algorithm based on Gaussian process (GP) learning is proposed to estimate the unknown channel between the UAV and the ground node. (3) To meet the real-time requirements when searching for the UAV's optimal relay position, two algorithms are proposed to reduce the search space. Specifically, for point-to-point communication, we propose a line search algorithm, and its effectiveness and stability are given and proved; for multi-node communication, we propose a general gradient-based algorithm to replace the global search.

The rest of this article is organized as follows: Section 1 presents the various models used in this article and the mathematical formulation of the UAV relay problem; Section 2 provides a detailed analysis of using the Gaussian process learning-based algorithm to estimate the unknown channel parameters between the UAV and the ground node; Section 3 proposes low-complexity solutions searching the optimal UAV relay position under two relay scenarios; Section 4 simulates the proposed relay motion-control algorithm in different application scenarios and conducts various comparisons and analyses. Finally, Section 5 summarizes the work of this article.

2. System Model and Problem Formulation

2.1. Air-to-Ground Relay Scenario in Urban Environments

As illustrated in Figure 1, multiple unmanned ground vehicles (UGVs) perform tasks (such as reconnaissance or search tasks) in area $\boldsymbol{\Omega} \in \mathrm{R}^2$. Due to the influence of surrounding buildings, trees, and terrain, the communication conditions between UGVs are poor. To improve the communication between UGVs, UAVs equipped with higher-performance communication equipment act as relays over the city. In Figure 1, blue rectangular prisms of different heights represent buildings in the city, red solid lines represent the communication links between relay UAVs and UGVs, cyan solid lines represent the flight trajectories of UAVs, and black dashed lines represent the motion trajectories of UGVs.

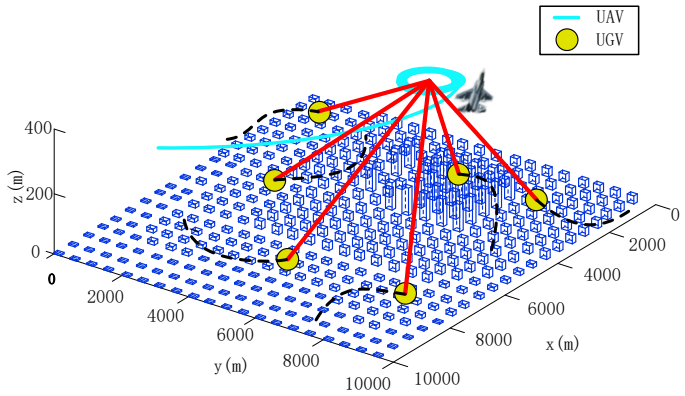

Figure 1. Illustration of air-to-ground relay communication scenario in urban environments.

Due to the complex and ever-changing urban environments in which UGVs are located, it is difficult to fully acquire the RF channel parameters of the entire task area before the relay task is executed. Therefore, the wireless channel parameters of the environments are unknown in advance. The UAV needs to estimate the wireless channel parameters near the current position in real time based on the online measured information and then calculate the optimal relay position and drive the UAV to fly to the optimal point, thereby providing the best possible communication link quality for the UGVs that are performing tasks.

2.2. UAV Kinematic Model

Assuming that the UAV is a fixed-wing aircraft and maintains a specific cruising altitude during the relay process, the control variables are the turning rate and acceleration. Let $\boldsymbol{p}_{\mathrm{u}} = [x_{\mathrm{u}}, y_{\mathrm{u}}]^{\mathrm{T}}$ represent the position vector, and the velocity vector is $[\dot{x}_{\mathrm{u}}, \dot{y}_{\mathrm{u}}]^{\mathrm{T}}$; then, its kinematic model can be expressed as [22]

$$\begin{cases} \dot{x}_{\mathrm{u}}(t) = v_{\mathrm{u}}(t)\cos\psi_{\mathrm{u}}(t) \\ \dot{y}_{\mathrm{u}}(t) = v_{\mathrm{u}}(t)\sin\psi_{\mathrm{u}}(t) \\ \dot{v}_{\mathrm{u}}(t) = a_{\mathrm{u}}(t) \\ \dot{\psi}_{\mathrm{u}}(t) = \frac{v_{\mathrm{u}}(t)}{r_{\mathrm{u}}(t)} = v_{\mathrm{u}}(t)c_{\mathrm{u}}(t) = \omega_{\mathrm{u}}(t) \end{cases} \tag{1}$$

where ψ_{u} is the heading angle, $\psi_{\mathrm{u}} \in [0, 2\pi)$; v_{u} is the flight speed, $v_{\mathrm{u}} = \|\boldsymbol{v}_{\mathrm{u}}\| = \left\|(\dot{x}_{\mathrm{u}}, \dot{y}_{\mathrm{u}})\right\|$; r_{u} is the turning radius, and $r_{\mathrm{u}} = \frac{1}{c_{\mathrm{u}}}$; a_{u} is the acceleration; ω_{u} is the turning rate, satisfying $|\omega_{\mathrm{u}}| \leq \omega_{\mathrm{u,max}}$. Due to the limitation of the aircraft's operating performance, the maximum turning rate $\omega_{\mathrm{u,max}}$ is constrained by the maximum roll angle $\psi_{\mathrm{u,max}}$, that is, $\omega_{\mathrm{u,max}} = \frac{g\tan(\psi_{\mathrm{u,max}})}{v_{\mathrm{u}}}$, where g is the acceleration constant under gravity.

This model assumes that the inner-loop control system of the UAV can quickly reach the required acceleration and turning rate, thus ignoring jerk and rolling inertia, and ignoring the influence of wind on the aircraft motion. In addition, this article assumes that the UAV maintains a specific speed during the relay process, the acceleration is 0, and the flight control variable is only the turning rate of the UAV.

2.3. Motion Model of the UGV

Although the Random Direction (RD) model and the Random Waypoint (RWP) model have been widely used in previous MANET research, the smooth turning (ST) motion model proposed by Wan et al. [23] has stronger generality and practicality, and it has begun to be used in the latest MANET-related research. Its two-dimensional mathematical model is as follows:

$$\begin{cases} a_{\mathrm{t}}(t) = \frac{dv_g}{dt} = 0 \\ a_{\mathrm{n}}(t) = \frac{v_g^2}{r(T_i)} \\ \dot{\psi}_g(t) = -\omega_g(t) = -\frac{v_g}{r(T_i)} \\ \dot{x}_g(t) = v_{g,x}(t) = v_g \cos(\psi_g(t)) \\ \dot{y}_g(t) = v_{g,y}(t) = v_g \sin(\psi_g(t)) \\ \tau(T_i) = T_{i+1} - T_i \end{cases} \quad T_i \le t < T_{i+1} \tag{2}$$

where $x_g(t)$ and $y_g(t)$ denote the coordinates of the node in the x and y direction at time t, respectively, i.e., $\boldsymbol{p}_g = [x_g(t), y_g(t)]^{\mathrm{T}}$; $v_{g,x}(t)$ and $v_{g,y}(t)$ respectively denote the velocity of the node in the x and y direction, that is, $\boldsymbol{v}_g = [v_{g,x}(t), v_{g,y}(t)]^{\mathrm{T}}$; $\omega_g(t)$ represents the turning rate of the node; $\psi_g(t)$ represents the heading angle; $a_{\mathrm{t}}(t)$ represents the vertical acceleration; $a_{\mathrm{n}}(t)$ represents the horizontal acceleration; $r(T_i)$ represents the turning radius selected at the T_i decision time; and $\tau(T_i)$ is the interval time.

2.4. Future Position Prediction Based on Kalman Filter

Due to the inability of the UAV to obtain the location of the UGV at the future moment, this paper uses the current position of the UGV obtained and represents the position change of the UGV through an Auto-Regressive (AR) motion model, and it then predicts the position of the node at the next moment based on the Kalman Filter (KF).

Let $\boldsymbol{x}_i(k) = [x_{i,k}, \dot{x}_{i,k}, \ddot{x}_{i,k}, y_{i,k}, \dot{y}_{i,k}, \ddot{y}_{i,k}]^{\mathrm{T}}$ represent the state of the UGV n_i at time k. $x_{i,k}$, $\dot{x}_{i,k}$, $\ddot{x}_{i,k}$ and $y_{i,k}$, $\dot{y}_{i,k}$, $\ddot{y}_{i,k}$ respectively represent the coordinates, velocity, and acceleration of the UGV n_i in the corresponding direction. Then, the state-transition equation of the UGV from time k to time $k+1$ can be expressed as follows:

$$\boldsymbol{x}_i(k+1) = \boldsymbol{F}\boldsymbol{x}_i(k) + \boldsymbol{\eta}_i(k) \tag{3}$$

$$\boldsymbol{F} = \begin{pmatrix} 1 & T_s & q_1 & 0 & 0 & 0 \\ 0 & 1 & q_2 & 0 & 0 & 0 \\ 0 & 0 & e^{-\alpha T_s} & 0 & 0 & 0 \\ 0 & 0 & 0 & 1 & T_s & q_1 \\ 0 & 0 & 0 & 0 & 1 & q_2 \\ 0 & 0 & 0 & 0 & 0 & e^{-\alpha T_s} \end{pmatrix} \tag{4}$$

$$q_1 = (e^{-\alpha T_s} + \alpha T_s - 1)/\alpha^2 \tag{5}$$

$$q_2 = (1 - e^{-\alpha T_s})/\alpha \tag{6}$$

where $\boldsymbol{F}$ denotes the transition matrix, and $\boldsymbol{\eta}_i(k)$ denotes the process noise, represented by a Gaussian variable with a mean of 0 and a covariance matrix $\boldsymbol{Q}_i(k) = \sigma_\eta^2 \boldsymbol{I}_6$, where $\boldsymbol{I}_6$ is a 6×6 unit matrix; T_s is the time interval from time k to time $k+1$; and α is a parameter used to simulate different types of maneuvering targets. When the speed is slow, α is small, and when the speed is fast, α is large. The noisy observation of the position of the UGV n_i at time k is [24]

$$\boldsymbol{p}_i(k) = \boldsymbol{H}\boldsymbol{x}_i(k) + \boldsymbol{v}_i(k) \tag{7}$$

$$\boldsymbol{H} = \begin{pmatrix} 1 & 0 & 0 & 0 & 0 & 0 \\ 0 & 0 & 0 & 1 & 0 & 0 \end{pmatrix} \tag{8}$$

where $\boldsymbol{p}_i(k)$ is the coordinate position of the UGV n_i observed at time k; $\boldsymbol{H}$ denotes the observation matrix; and $\boldsymbol{v}_i(k)$ denotes the observation noise, represented by a Gaussian variable with a mean of 0 and a covariance matrix $\boldsymbol{R}_i(k) = \sigma_v^2 \boldsymbol{I}_2$, where $\boldsymbol{I}_2$ denotes a 2×2 unit matrix. Therefore, the position filtering and prediction process of the UGV n_i can be given as $\hat{\boldsymbol{x}}_{i,k|k-1} = \boldsymbol{F}\hat{\boldsymbol{x}}_{i,k-1}$ and $\boldsymbol{L}_{i,k|k-1} = \boldsymbol{F}\boldsymbol{L}_{i,k-1}\boldsymbol{F}^{\mathrm{T}} + \boldsymbol{Q}_{i,k-1}$, where subscript i represents the i-th ground node; $\hat{\boldsymbol{x}}_{i,k-1}$ is the estimated state value of ground node i at time $k-1$; $\hat{\boldsymbol{x}}_{i,k|k-1}$ is the estimated state value of ground node i at time k based on the state value at

time $k-1$. Kalman gain can be expressed as $\boldsymbol{K}_{i,k} = \boldsymbol{L}_{i,k|k-1}\boldsymbol{T}^{\mathrm{T}}(\boldsymbol{T}\boldsymbol{L}_{i,k|k-1}\boldsymbol{T}^{\mathrm{T}} + \boldsymbol{R}_{i,k})^{-1}$. State measurement and covariance matrix can be given as $\hat{\boldsymbol{x}}_{i,k} = \hat{\boldsymbol{x}}_{i,k|k-1} + \boldsymbol{K}_{i,k}(\boldsymbol{p}_{i,k} - \boldsymbol{T}\hat{\boldsymbol{x}}_{i,k|k-1})$ and $\boldsymbol{L}_{i,k} = (\boldsymbol{I}_4 - \boldsymbol{K}_{i,k}\boldsymbol{T})\boldsymbol{L}_{i,k|k-1}$. The corresponding derivation process can be found in [24].

2.5. Problem Formulation of Optimal Relay Position Search

This article drives the UAV to the desired relay position by controlling its motion, in order to achieve optimal network performance. Let $\boldsymbol{N} = \{n_1, n_2, \ldots, n_N\}$ be the set of UGVs, where N is the number of UGVs. Let $\boldsymbol{p}_i = [x_i, y_i]$, $i = 1, 2, \ldots, N$ represent the position of UGV n_i, and, assuming that the flight altitude and speed of the UAV remain constant (which is reasonable for many UAV relay tasks), then the flight control variable of the UAV is only the turning rate $\dot{\psi}_{\mathrm{u}}$. The goal of relay motion control is to optimize the objective function by finding the optimal value for the turning rate of the UAV. The problem model is established as follows:

$$\dot{\psi}_{\mathrm{u}}^{*} = \underset{|\dot{\psi}_{\mathrm{u}}| \le \omega_{\mathrm{u,max}}}{\mathrm{argmax}} J(\dot{\psi}_{\mathrm{u}}) \tag{9}$$

where $J(\dot{\psi}_u)$ represents the performance index function.

This article develops a decision system by determining the optimal UAV location, then uses the guidance law to drive the UAV to this location. We focus our research on the former issue and formulate it as follows:

$$\boldsymbol{p}_{\mathrm{u}}^{*} = \underset{\boldsymbol{p}_{\mathrm{u}} \in \boldsymbol{\Omega}}{\mathrm{argmax}} J(\boldsymbol{p}_u) \tag{10}$$

where $\boldsymbol{p}_{\mathrm{u}}^{*}$ denotes the optimal relay position.

2.6. Motion Control Framework for Relay UAV

This article aims to solve the issue of online autonomous motion control of relay UAVs in the case of supporting moving nodes, unknown RF channel parameters, and only RSS information. To solve the issue of inaccurate position and predicted positions of moving nodes, a method based on Kalman Filtering is established. To cope with the situation where RF channel parameters are unknown and only RSS and node position information are available, a channel parameter estimation method based on online collectible data is established, and a novel simplified optimal UAV position-calculation method is proposed. Finally, the optimal position is input to the UAV guidance flight module, which outputs the required turning rate to drive the UAV to fly to the optimal relay point, thereby optimizing the network performance. The corresponding method framework of this article is shown in Figure 2.

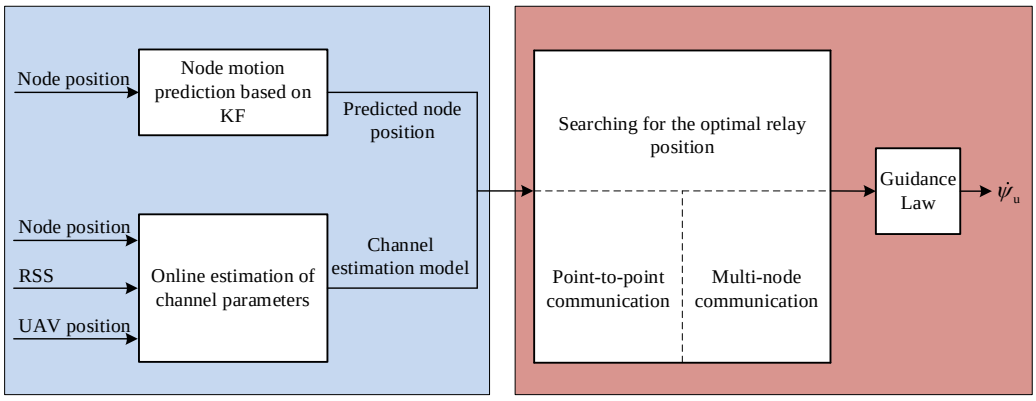

Figure 2. Motion control framework.

3. Online Estimation of Wireless Channel Parameters

In the air-to-ground relay system, the UGVs perform tasks (such as reconnaissance or search) in the environmental area, while the UAV dynamically adjusts its positions according to the movements of the UGVs and changes in the RF signal environment, so as to continuously provide the best possible communication performance for the UGVs.

This problem mainly involves two aspects, namely, communication and motion control, which are closely related and coupled with each other because the quality of communication determines the UAV's motion direction and position of the next moment, and the motion of nodes will influence the communication performance of the entire network.

3.1. Model of the Received Signal

Previous studies on UAV relay communication have mostly adopted relatively simple channel models, resulting in reduced communication performance. This paper studies the air-to-ground relay system under urban environments, where the RF signal environment is more complex. Therefore, it is necessary to adopt a more realistic communication model.

Assume that the UAV u and N UGVs $n_i \in N = \{n_1, n_2, \ldots, n_N\}$ in the task area $\boldsymbol{\Omega}$ are equipped with omnidirectional antennas. As shown in Figure 3, air-to-ground signal propagation is divided into two parts: free space and low-altitude environment. In the low-altitude environment, due to the existence of buildings, trees, and other obstacles, the signal undergoes shadowing and scattering phenomena, thereby introducing extra loss in the air-to-ground transmission link. The channel fading between the relay UAV and the UGV can be modeled as [25,26]

$$P_{r,i} = P_{t,i} - L_i - \Psi_i \tag{11}$$

$$L_i = 10\lambda \log_{10}\left(\frac{4\pi f_c d_i}{c}\right) \tag{12}$$

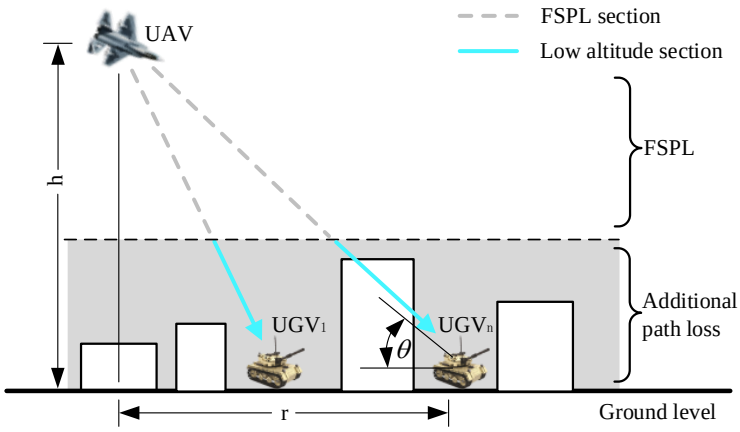

Figure 3. Schematic diagram of air-to-ground signal propagation.

In Equation (16), $P_{r,i}$ represents the power received by the UAV u from the i-th UGV n_i, in dBm; $P_{t,i}$ represents the signal transmission power of n_i, in dBm; L_i represents the path fading loss between u and n_i, in dB; and Ψ_i represents the shadow fading loss between u and n_i, in dB.

In Equation (17), d_i represents the distance between u and n_i; f_c represents the carrier frequency of the radio wave; c represents the speed of the light wave; and λ represents the path attenuation factor, generally ranging from 2 to 6.

In air-to-ground communication, the density of buildings has a great influence on the channel characteristics. This is because their distribution characteristics affect the probability of the LoS (Line of Sight) component. Due to the movement of UGVs, this probability is prone to sudden changes, such as if the LoS between the UGV and the relay UAV is suddenly blocked by a high building. Obviously, the simple distance channel model

(DCM) [27] and the statistical distribution-based probabilistic channel model (SDPCM) [28] cannot reflect the impact of the above factors. In addition, the flight altitude of the UAV affects the elevation angle of the LoS between the UGV and the UAV, which in turn affects the LoS probability. The DCM and the SDPCM are also difficult to reflect the impact of altitude on channel characteristics.

To calculate the expected value of shadow fading between the relay UAV and the UGV with an elevation angle of θ, the following equation can be applied to obtain [25,26]:

$$\Psi_i = \sum_{\varepsilon} \eta_\varepsilon P(\varepsilon, \theta) \tag{13}$$

where $P(\varepsilon, \theta)$ is the probability of the ε-th signal propagation group with an elevation angle of θ, and η_ε denotes the shadow fading loss value of the ε-th propagation group. This study follows the assumption of two propagation groups, strictly corresponding to the LoS propagation condition and the NLoS (None Line of Sight) propagation condition, that is, when $\varepsilon \in \{\text{LoS}, \text{NLoS}\}$, then [29]

$$\Psi = P(\text{LoS}, \theta)\eta_{\text{LoS}} + (1 - P(\text{LoS}, \theta))\eta_{\text{NLoS}} \tag{14}$$

where η_{LoS} and η_{NLoS} denote the additional path loss of the LoS link and the NLoS link, respectively.

The LoS probability is affected by the environment and is a function of the transmitting antenna height h_{TX} and the receiving antenna height h_{RX}. It is also related to the statistical parameters of the environment. According to the recommendations document of the International Telecommunication Union, it can be formulated as follows [30]:

$$P(\text{LoS}) = \prod_{n=0}^{m} \left[1 - \exp\left(-\frac{\left[h_{\text{TX}} - \frac{(n + \frac{1}{2})(h_{\text{TX}} - h_{\text{RX}})}{m+1} \right]^2}{2\gamma^2} \right) \right] \tag{15}$$

$$m = \text{floor}(r\sqrt{\alpha\beta} - 1) \tag{16}$$

where α represents the percentage of the building land to the total land; β represents the number of buildings per square kilometer; γ is the proportional parameter describing the building height distribution; and r denotes the ground distance between the transmitting antenna and the receiving antenna, as illustrated in Figure 3. Since the receiving antenna height h_{RX} is much lower than the height of the building and the relay UAV, it can be ignored. Therefore, the ground distance r between the relay UAV and the UGV is calculated as follows:

$$r = \frac{h}{\tan(\theta)} \tag{17}$$

where h denotes the UAV's altitude. By fitting the channel attenuation of Equation (20) in different environments, it can be found that Equation (20) can be expressed by the Sigmoid function (S-Curve), as follows [25]:

$$P(\text{LoS}, \theta) = \frac{1}{1 + a\exp(-b(\theta - a))} \tag{18}$$

$$\theta = \frac{180}{\pi} \times \arctan\left(\frac{h}{r}\right) \tag{19}$$

where a and b are S-Curve parameters, and θ denotes the elevation angle, as shown in Figure 3.

Since the communication model used in this article takes into account the impact of the environment on the LoS signal component, that is, simultaneously considering the probability of the occurrence of LoS channels and NLoS channels, it will be referred to as the average gain-based probability channel model (AGPCM) in the following.

3.2. Channel Estimation Based on Gaussian Process

In practical application, it is difficult or even impractical to acquire the RF channel parameters of the entire task area before the relay task due to the dynamics of the network, the differences in the nodes, the changes in the RF distribution in the task area, etc. Gaussian process (GP) is mainly utilized to infer or predict the function value on finite test points based on observed data. Therefore, this article proposes a GP-based learning algorithm that utilizes online collected RSS data to learn the impact of shadow fading and combines it with the known parts of the communication model.

From Equation (16), it can be seen that the received power $P_{r,i}$ is related to the signal transmission power $P_{t,i}$, path fading L_i, and shadow fading Ψ. Since $P_{t,i}$ is a constant, and the path fading L_i is caused by the continuous consumption of the transmitted signal as the propagation distance increases, and from Equation (17), it can be seen that L_i is constant at a specific location, so only the shadow fading Ψ needs to be estimated.

Shadow fading Ψ is caused by obstacles between the transmitter and receiver. When modeling shadow fading in an environment with incomplete information, it is generally assumed that the channel gain follows a Gaussian distribution with variance σ^2, that is [31],

$$\Psi \sim N(\mu, \sigma^2) \tag{20}$$

where μ represents the fading mean, and σ^2 represents the fading variance.

GP is a random process defined on a continuous domain. For this article, the continuous domain is a small spatial domain around the current position of the UAV, denoted as $\boldsymbol{\delta}$. Let t_k denote the decision moment; in a given environment, the wireless channel is sparsely sampled at the node positions $\boldsymbol{P}_i = \{\boldsymbol{p}_i^1, \boldsymbol{p}_i^2, \ldots, \boldsymbol{p}_i^\kappa\} \subset \boldsymbol{\Omega}$, $i = 1, 2,...,N$ during time $[t_{k-1}, t_k)$, where κ is the number of samples. Those channel measurements can be performed by the UAV along its trajectory $\boldsymbol{P}_\mathrm{u} = \{\boldsymbol{p}_\mathrm{u}^1, \boldsymbol{p}_\mathrm{u}^2, \ldots, \boldsymbol{p}_\mathrm{u}^\kappa\} \subset \boldsymbol{\Omega}$. Since the UAV maintains a constant altitude when performing the relay task, any position $\boldsymbol{p}$ in the continuous domain $\boldsymbol{\delta}$ can be regarded as a two-dimensional vector. For the convenience of the subsequent process, $\boldsymbol{p}$ is re-recorded as $\boldsymbol{x} \in R^2$, then the κ input features constitute $\boldsymbol{X} = [\boldsymbol{x}_1, \boldsymbol{x}_2, \ldots, \boldsymbol{x}_\kappa]^\mathrm{T}$, $\boldsymbol{X} \in R^{\kappa \times 2}$, and the corresponding target value $\boldsymbol{y} = [y_1, y_2, \ldots, y_\kappa]^\mathrm{T}$, $\boldsymbol{y} \in R^{\kappa \times 1}$, $\boldsymbol{y}$ represents the vector of received signal power measurement, so the training set can be formulated as $\boldsymbol{D} = \{(\boldsymbol{X}, \boldsymbol{y})\}$. Considering that the actual output contains noise, the Gaussian process regression is modeled as follows:

$$\begin{cases} y_i = f(\boldsymbol{x}_i) + \varepsilon & i = 1, 2, \ldots, \kappa \\ \varepsilon \sim N(0, \overline{\sigma}_n^2) \end{cases} \tag{21}$$

where ε is Gaussian white noise with a mean of 0 and a variance of $\overline{\sigma}_n^2$, and $f(\cdot)$ represents an implicit function independent of the noise. Assuming that the function value $f(\boldsymbol{x}_1)$, $f(\boldsymbol{x}_2)$, ..., $f(\boldsymbol{x}_\kappa)$ forms a joint Gaussian distribution after the input feature is mapped by function f, since the noise ε and the implicit function f are independent of each other, the output y_i also obeys a Gaussian distribution, and the set of its finite observations' joint distributions can form a GP, that is [31],

$$y \sim GP(m(\boldsymbol{x}), k(\boldsymbol{x}', \boldsymbol{x})) \tag{22}$$

$$m(\boldsymbol{x}) = E[f(\boldsymbol{x})] \tag{23}$$

$$k(\boldsymbol{x}', \boldsymbol{x}) = E[(f(\boldsymbol{x}) - m(\boldsymbol{x}))(f(\boldsymbol{x}') - m(\boldsymbol{x}'))] \tag{24}$$

where $m(\boldsymbol{x})$ denotes the mean function of the implicit function $f(\boldsymbol{x})$, and $k(\boldsymbol{x}', \boldsymbol{x})$ denotes the covariance function of the implicit function $f(\boldsymbol{x})$. Since the space of the urban environment where the UAV performs the relay task is irregular, the radial basis function (RBF) can realize nonlinear mapping, and the hyperparameters required for training are greatly reduced compared to the polynomial kernel function, RBF is used in this paper to characterize the covariance function [32]:

$$k(\boldsymbol{x}', \boldsymbol{x}) = \sigma_f^2 \exp\left[-\frac{1}{2}(\boldsymbol{x} - \boldsymbol{x}')^{\mathrm{T}} \boldsymbol{M}_{\mathrm{D}} (\boldsymbol{x} - \boldsymbol{x}')\right] \tag{25}$$

where $\boldsymbol{M}_{\mathrm{D}} = \mathrm{diag}(l^2)$ is a symmetric matrix about the hyperparameter l, where l is the horizontal factor parameter; the hyperparameter σ_f^2 is the vertical scale factor that regulates the variation of the covariance function. Then, define the mean function as:

$$m(\boldsymbol{x}) = c \tag{26}$$

where c denotes the hyperparameter to be optimized. Let $\boldsymbol{\theta} = [l, \sigma_f^2, c]$ be the hyperparameter set, and the optimal value needs to be obtained through training and learning. Under the condition that the channel fading in each sampling satisfies independence, the fitness of the GP model to the training set $\boldsymbol{D}$ can be evaluated by the following marginal likelihood conditioned on the hyperparameter set $\boldsymbol{\theta}$:

$$\begin{array}{l} L(\boldsymbol{\theta}) = \log(\boldsymbol{y}|\boldsymbol{X}, \boldsymbol{\theta}) = -\frac{1}{2}\boldsymbol{y}^{\mathrm{T}}(\boldsymbol{K}_{XX} + \sigma_n^2 \boldsymbol{I})^{-1}\boldsymbol{y} \\ -\frac{1}{2}\log|\boldsymbol{K}_{XX} + \sigma_n^2 \boldsymbol{I}| - \frac{\kappa}{2}\log(2\pi) \end{array} \tag{27}$$

Therefore, the hyperparameter set $\boldsymbol{\theta}$ of the GP model can be obtained through maximizing the marginal likelihood $L(\boldsymbol{\theta})$, that is [33],

$$\boldsymbol{\theta}^* = \underset{\boldsymbol{\theta}}{\mathrm{argmax}}(L(\boldsymbol{\theta})) \tag{28}$$

According to the Bayesian principle, the GP model establishes a priori function in the training set $\boldsymbol{D}$ and converts it into a posterior distribution on the test data $\boldsymbol{x}^*$. Therefore, the prediction result y^* obtained from the test data input forms a joint Gaussian distribution with the target value $\boldsymbol{y}$ of the training set data, that is,

$$\begin{bmatrix} \boldsymbol{y} \\ y^* \end{bmatrix} \sim N\left(\begin{bmatrix} \boldsymbol{\mu}(\boldsymbol{X}) \\ \mu(\boldsymbol{x}^*) \end{bmatrix}, \begin{bmatrix} \boldsymbol{K}_{XX} + \sigma_n^2 \boldsymbol{I} & \boldsymbol{K}_{Xx^*} \\ \boldsymbol{K}_{x^*X} & \boldsymbol{K}_{x^*x^*} \end{bmatrix}\right) \tag{29}$$

where $\boldsymbol{K}_{XX}$ represents the autocovariance matrix of the input features of the training set; $\boldsymbol{K}_{x^*x^*}$ represents the autocovariance matrix of the input features of the test set; and $\boldsymbol{K}_{Xx^*}$ represents the covariance matrix between the input features of the training set data and the test set data. For $\boldsymbol{x}^*$, the prediction result based on the GP model is as follows:

$$y^*|\boldsymbol{X}, \boldsymbol{y} \sim N(\mu_{f|X,y}(\boldsymbol{x}^*), \sigma_{f|X,y}^2(\boldsymbol{x}^*)) \tag{30}$$

$$\mu(\boldsymbol{x}^*) = \boldsymbol{K}_{x^*X}(\boldsymbol{K}_{XX} + \sigma_n^2 \boldsymbol{I})^{-1}(\boldsymbol{y} - \boldsymbol{\mu}(\boldsymbol{X})) + \mu(\boldsymbol{x}^*) \tag{31}$$

$$\sigma^2(\boldsymbol{x}^*) = \boldsymbol{K}_{x^*x^*} - \boldsymbol{K}_{x^*X}(\boldsymbol{K}_{XX} + \sigma_n^2 \boldsymbol{I})^{-1}\boldsymbol{K}_{x^*X} \tag{32}$$

where $\mu(\boldsymbol{x}^*)$ denotes the mean of y^*, and $\sigma^2(\boldsymbol{x}^*)$ denotes the variance of y^*. The optimal value of the hyperparameters of the GP model is solved by Equation (33), and then, the mean and variance of the predicted output results are obtained using Equations (36) and (37), which are the mean and variance of the shadow fading at any position $\boldsymbol{x}^* \in \boldsymbol{\delta}$ near the current position of the UAV.

It should be pointed out that since both the UAV and the UGVs are moving, the RF distribution characteristics are actually changing dynamically. Therefore, the wireless

channel parameter-estimation method proposed in this article can only estimate the channel characteristics near the UAV and cannot estimate the channel characteristics of the entire task area.

4. Searching for the Optimal Relay Position

This section presents and analyzes the adaptive optimal relay position search algorithm, which aims to give the optimal relay point, including point-to-point communication and multi-node communication.

4.1. Point-to-Point Communication

In point-to-point communication, UAVs play the role of forwarding information between two nodes that cannot communicate directly (such as a control station and a remote task node), thereby realizing indirect information exchange between the two. Due to the weaker communication capability of the ground node compared to the relay UAV, the performance bottleneck of the link lies in the uplink channel from the ground node to the relay UAV. Therefore, in point-to-point communication, the optimization of UAV position can be transformed into the following form:

$$\boldsymbol{p}_{\mathrm{u}}^{*} = \arg\max_{\boldsymbol{p}_{\mathrm{u}} \in \boldsymbol{\Omega}} \min\left\{S_{\boldsymbol{p}_1,\boldsymbol{p}_{\mathrm{u}}}, S_{\boldsymbol{p}_2,\boldsymbol{p}_{\mathrm{u}}}\right\}, \quad \boldsymbol{p}_1, \boldsymbol{p}_2 \in \boldsymbol{N} \tag{33}$$

where $S_{\boldsymbol{p}_i,\boldsymbol{p}_{\mathrm{u}}}$ represents the strength of the wireless signal sent by the node n_i at position $\boldsymbol{p}_i$ and received by the relay UAV u at position $\boldsymbol{p}_{\mathrm{u}}$, and $J = \min\left\{S_{\boldsymbol{p}_1,\boldsymbol{p}_{\mathrm{u}}}, \ S_{\boldsymbol{p}_2,\boldsymbol{p}_{\mathrm{u}}}\right\}$ represents the communication index function under point-to-point communication, which is constrained by the link with the worst power. Moreover, the larger the value of J, the better the network performance.

The necessary condition for the objective function $J = \min\left\{S_{\boldsymbol{p}_1,\boldsymbol{p}_{\mathrm{u}}}, S_{\boldsymbol{p}_2,\boldsymbol{p}_{\mathrm{u}}}\right\}$ in Equation (38) to achieve the maximum value is that $\boldsymbol{p}_{\mathrm{u}}^{*}$ satisfies the following equation:

$$\nabla J(\boldsymbol{p}_{\mathrm{u}}^{*}) = \frac{\partial J}{\partial \boldsymbol{p}_{\mathrm{u}}} \mid_{\boldsymbol{p}_{\mathrm{u}} = \boldsymbol{p}_{\mathrm{u}}^{*}} = 0 \tag{34}$$

In Equation (38), $\min(\cdot)$ indicates that the objective function J is non-smooth and needs segmented differentiation according to the values of $S_{\boldsymbol{p}_1,\boldsymbol{p}_{\mathrm{u}}}$ and $S_{\boldsymbol{p}_2,\boldsymbol{p}_{\mathrm{u}}}$, as follows:

$$\nabla J = \begin{cases} \nabla S_{\boldsymbol{p}_1,\boldsymbol{p}_{\mathrm{u}}}, & \text{if } S_{\boldsymbol{p}_1,\boldsymbol{p}_{\mathrm{u}}} < S_{\boldsymbol{p}_2,\boldsymbol{p}_{\mathrm{u}}} \\ \nabla S_{\boldsymbol{p}_2,\boldsymbol{p}_{\mathrm{u}}}, & \text{if } S_{\boldsymbol{p}_1,\boldsymbol{p}_{\mathrm{u}}} > S_{\boldsymbol{p}_2,\boldsymbol{p}_{\mathrm{u}}} \\ \text{Other}, & \text{if } S_{\boldsymbol{p}_1,\boldsymbol{p}_{\mathrm{u}}} = S_{\boldsymbol{p}_2,\boldsymbol{p}_{\mathrm{u}}} \end{cases} \tag{35}$$

Theorem 1. *Solving $\boldsymbol{p}_{\mathrm{u}}^{*}$ is equivalent to finding $\boldsymbol{p}_{\mathrm{u}}$ that satisfies both of the following conditions simultaneously: (1) $S_{\boldsymbol{p}_1,\boldsymbol{p}_{\mathrm{u}}} = S_{\boldsymbol{p}_2,\boldsymbol{p}_{\mathrm{u}}}$; (2) $\boldsymbol{p}_{\mathrm{u}} = \boldsymbol{p}_1 + \alpha\ (\boldsymbol{p}_2 - \boldsymbol{p}_1)$, where $0 < \alpha < 1$.*

Proof. Condition (2) indicates that the optimal relay position $\boldsymbol{p}_{\mathrm{u}}^{*}$ must be on the line segment $[\boldsymbol{p}_1, \boldsymbol{p}_2]$ bounded by the two point-to-point node positions $\boldsymbol{p}_1$ and $\boldsymbol{p}_2$. The proof process is divided into two aspects. □

The sufficiency proof of the theorem states that if $\boldsymbol{p} = \boldsymbol{p}^{*}$, then $S_1(\boldsymbol{p}) = S_2(\boldsymbol{p})$ and $\boldsymbol{p} = \boldsymbol{p}_1 + \alpha\ (\boldsymbol{p}_2 - \boldsymbol{p}_1)$.

First, we assume that $S_1(\boldsymbol{p}) > S_2(\boldsymbol{p})$. From Equation (40), we know that $\nabla J = \nabla S_2(\boldsymbol{p})$, then $\nabla S_2(\boldsymbol{p}) = 0$, the condition for $\nabla S_2(\boldsymbol{p}) = 0$ is $d_2 = 0$ (d_2 represents the Euclidean distance between $\boldsymbol{p}_2$ and $\boldsymbol{p}$). However, $S_i(\boldsymbol{p})$ is inversely proportional to the distance d_i, that is, $S_1(\boldsymbol{p}) > S_2(\boldsymbol{p})$ means that the distance $d_1 < d_2$, so $d_1 < 0$, which obviously does not conform to the actual situation, and the assumption is not valid. Similarly, $S_1(\boldsymbol{p}) \not< S_2(\boldsymbol{p})$. Therefore, $S_1(\boldsymbol{p}) = S_2(\boldsymbol{p})$.

Next, we assume $\boldsymbol{p}_{\mathrm{u}}^{*} \notin [\boldsymbol{p}_1, \boldsymbol{p}_2]$. Obviously, there is a point $\boldsymbol{p}' \in [\boldsymbol{p}_1, \boldsymbol{p}_2]$ that satisfies $S_{\boldsymbol{p}_1,\boldsymbol{p}'} = S_{\boldsymbol{p}_2,\boldsymbol{p}'}$, while $\boldsymbol{p}'$ is not the optimal relay point. Therefore, $S_{\boldsymbol{p}_1,\boldsymbol{p}} = S_{\boldsymbol{p}_2,\boldsymbol{p}} \geq S_{\boldsymbol{p}_1,\boldsymbol{p}'} = S_{\boldsymbol{p}_2,\boldsymbol{p}'}$, so $d_{\boldsymbol{p}_1,\boldsymbol{p}} \leq d_{\boldsymbol{p}_1,\boldsymbol{p}'}$ and $d_{\boldsymbol{p}_2,\boldsymbol{p}} \leq d_{\boldsymbol{p}_2,\boldsymbol{p}'}$, and then $d_{\boldsymbol{p}_1,\boldsymbol{p}} + d_{\boldsymbol{p}_2,\boldsymbol{p}} \leq d_{\boldsymbol{p}_1,\boldsymbol{p}'} + d_{\boldsymbol{p}_2,\boldsymbol{p}'}$. According to the triangle's characteristic that the sum of the lengths of two sides must be greater than the length of the third side, this does not conform to the actual situation, that is, the assumption is not valid. Therefore, there must be $\boldsymbol{p}_{\mathrm{u}}^{*} \in [\boldsymbol{p}_1, \boldsymbol{p}_2]$.

In summary, the sufficiency of the theorem has been proven. The next step is to prove the necessity of the theorem, that is, if $S_{\boldsymbol{p}_1,\boldsymbol{p}_{\mathrm{u}}} = S_{\boldsymbol{p}_2,\boldsymbol{p}_{\mathrm{u}}}$ and $\boldsymbol{p}_{\mathrm{u}} \in [\boldsymbol{p}_1, \boldsymbol{p}_2]$, then $\boldsymbol{p}_{\mathrm{u}} = \boldsymbol{p}_{\mathrm{u}}^{*}$.

We assume that there is a point $\boldsymbol{p}'$ that satisfies $S_{\boldsymbol{p}_1,\boldsymbol{p}'} = S_{\boldsymbol{p}_2,\boldsymbol{p}'}$ and $\boldsymbol{p}' \in [\boldsymbol{p}_1, \boldsymbol{p}_2]$, but $\boldsymbol{p}'$ is not the optimal UAV point. Because $\boldsymbol{p}_{\mathrm{u}}^{*}$ is the optimal UAV point, $S_{\boldsymbol{p}_1,\boldsymbol{p}_{\mathrm{u}}^{*}} = S_{\boldsymbol{p}_2,\boldsymbol{p}_{\mathrm{u}}^{*}} > S_{\boldsymbol{p}_1,\boldsymbol{p}'} = S_{\boldsymbol{p}_2,\boldsymbol{p}'}$, and therefore, $d_{\boldsymbol{p}_1,\boldsymbol{p}_{\mathrm{u}}^{*}} < d_{\boldsymbol{p}_1,\boldsymbol{p}'}$. Also, the value of $d_{\boldsymbol{p}_1,\boldsymbol{p}_2}$ is constant, $d_{\boldsymbol{p}_2,\boldsymbol{p}_{\mathrm{u}}^{*}} > d_{\boldsymbol{p}_2,\boldsymbol{p}'}$, resulting in $S_{\boldsymbol{p}_2,\boldsymbol{p}_{\mathrm{u}}^{*}} < S_{\boldsymbol{p}_2,\boldsymbol{p}'}$. This is contrary to the assumption that $S_{\boldsymbol{p}_2,\boldsymbol{p}_{\mathrm{u}}^{*}} > S_{\boldsymbol{p}_2,\boldsymbol{p}'}$ has been derived. Therefore, the assumption does not hold, that is, $\boldsymbol{p}' = \boldsymbol{p}_{\mathrm{u}}^{*}$ must be true, and the proof of Theorem 1 ends.

In Theorem 1, $\boldsymbol{p}_{\mathrm{u}}^{*}$ is only related to α. Therefore, the line search algorithm is able to be used to reduce the search space required to find the optimal UAV point under point-to-point communication.

Considering the possible situation, the relay UAV may still be unable to track changes in the optimal relay position point over time. Therefore, it is necessary to study the convergence conditions of this method:

Theorem 2. *When the speed of the UAV is greater than the maximum speed of the UGV, that is,* $v_{\mathrm{u}} > \max(v_1, v_2)$*, it can ensure that the UAV will converge to the optimal relay point.*

Proof. Let the changing speed of the optimal relay position point be $v_{\boldsymbol{p}}^{*}$. If the UAV can converge to $\boldsymbol{p}^{*}$, the constraint $v > v_{\boldsymbol{p}}^{*}$ must be met. According to the conclusion $\boldsymbol{p}^{*} = \boldsymbol{p}_1 + \alpha\ (\boldsymbol{p}_2 - \boldsymbol{p}_1)$ in Theorem 1, taking the derivative yields $\boldsymbol{v}^{*} = \boldsymbol{v}_1 + \alpha\ (\boldsymbol{v}_2 - \boldsymbol{v}_1)$, where $\alpha \in (0, 1)$, and obviously $v = \left\|\dot{\boldsymbol{p}}^{*}\right\| < \max\ (\ \|\boldsymbol{v}_1\|, \|\boldsymbol{v}_2\|\ )$, if $v > \max\ (\boldsymbol{v}_1, \boldsymbol{v}_2)$, then there must be $v > \|\boldsymbol{v}^{*}\|$, $\|\boldsymbol{v}^{*}\|$ is $\left\|\dot{\boldsymbol{p}}^{*}\right\|$, and Theorem 2 is proved. □

Theorem 2 reveals that as long as the UAV's speed is greater than the maximum speed of the UGV, the relay task can be guaranteed to be feasible.

4.2. Multi-Node Communication

For relay to support multi-node communication, each node in the ground system may need to utilize the relay-forwarding capability of the UAV to exchange information with other nodes, so the communication performance between all node pairs needs to be considered. The communication performance between nodes is usually limited by the uplink from the ground node to the relay, which contains multiple uplink channels with different transmission capabilities. Therefore, the objective function of the $\min(\cdot)$ form in Section 3.1 is no longer suitable as a metric to evaluate the communication performance of a multi-node relay network. This article uses the following objective function to characterize the network performance of multi-node communication [34]:

$$\boldsymbol{p}_{\mathrm{u}}^{*} = \arg\min_{\boldsymbol{p}_{\mathrm{u}} \in \boldsymbol{\Omega}} \frac{1}{N} \sum_{i=1}^{N} \frac{1}{S_{\boldsymbol{p}_i,\boldsymbol{p}_{\mathrm{u}}}}, \qquad n_i \in \boldsymbol{N} \tag{36}$$

where $\dfrac{1}{J} = \dfrac{1}{N} \sum\limits_{i=1}^{N} \dfrac{1}{S_{\boldsymbol{p}_i,\boldsymbol{p}_{\mathrm{u}}}}$, the network performance J represents the average power of all channels, and the larger the value of J, the better the network performance.

First, we discuss a special case where the attenuation factors of each channel satisfy the condition $\lambda_1 = \lambda_2 = \cdots = \lambda_N = 2$. By solving Equation (39) and (41), we can obtain the following:

$$x_u^* = \frac{\sum \frac{1}{G_i} x_i}{\sum \frac{1}{G_i}}, \qquad y_u^* = \frac{\sum \frac{1}{G_i} y_i}{\sum \frac{1}{G_i}} \tag{37}$$

where x_u^* and y_u^* are the coordinates of the optimal relay point, that is, $\boldsymbol{p}_{\mathrm{u}}^* = (x_u^*, y_u^*)$, and G_i denotes the communication channel gain between the relay UAV u and the UGV n_i.

However, in many practical applications, due to the diversity of nodes, the dynamics of the system, and changes in the environment, channel parameters do not meet the above conditions, that is, the assumption $\lambda_1 = \lambda_2 = \cdots = \lambda_N = 2$ is not satisfied. Solving Equation (41) is a very challenging issue, and this paper proposes a new gradient-based method to solve this issue, and it has a relatively small computational cost.

For each node n_i, $i = 1, 2, \ldots, N$ in the ground multi-vehicle system, the power $S_{\hat{\boldsymbol{p}}_i, \boldsymbol{p}'_{\mathrm{u}}(\beta)}$ emitted by the UGV n_i at $\hat{\boldsymbol{p}}_i$ and received by the relay UAV u at $\boldsymbol{p}'_{\mathrm{u}}(\beta) = \boldsymbol{p}_{\mathrm{u}} + [R\cos\beta, R\sin\beta\,]^{\mathrm{T}}$, $0 \le \beta < 2\pi$ can be estimated using the wireless channel estimation model in Section 2.2 (Equations (25)~(37)), where $\hat{\boldsymbol{p}}_i$ denotes the predicted position of the UGV n_i by the Kalman Filter, $\boldsymbol{p}_{\mathrm{u}}$ represents the UAV's current position, and R represents a constant distance from $\boldsymbol{p}_{\mathrm{u}}$. Therefore, the objective function J of the network performance in Equation (41) is updated as follows:

$$\frac{1}{J(\beta)} = \frac{1}{N} \sum_{i=1}^{N} \frac{1}{S_{\hat{\boldsymbol{p}}_i, \boldsymbol{p}'_{\mathrm{u}}(\beta)}}, \qquad 0 \le \beta < 2\pi \tag{38}$$

The positive gradient direction β^* is the direction in which the objective function rises fastest. Therefore, according to Equation (43), β^* can be calculated by maximizing the objective function $J(\beta)$, that is,

$$\beta^* = \arg \max_{\beta \in [0, 2\pi)} J(\beta) \tag{39}$$

After calculating the positive gradient direction β^* near the current position of the relay UAV, the unit direction vector of the optimal target position of the UAV at the next moment can be formulated as follows:

$$\boldsymbol{\mu}_{t_k} = (\cos\beta^*, \sin\beta^*) \tag{40}$$

According to the basic principle of the gradient climbing method, the optimal target position for the next moment can be calculated from the current position $\boldsymbol{p}_{\mathrm{u}}$ and the optimal unit direction vector $\boldsymbol{\mu}_{t_k}$, as follows:

$$\boldsymbol{p}_{\mathrm{u},t_k}^* = \boldsymbol{p}_{\mathrm{u}} + \gamma \cdot \boldsymbol{\mu}_{t_k} \tag{41}$$

where γ is a predefined dimensionless quantity.

5. Simulation Results and Analysis

This section uses simulation experiments to verify and analyze the feasibility of the proposed online autonomous motion control method for relay UAV supporting UGVs' communication in urban environments, as well as to compare algorithm performance. This experiment considers the scenario of UAV supporting point-to-point communication and multi-node communication for UGVs, and gradually shifts from discussing supporting stationary nodes to moving nodes and then to moving nodes in unknown channels.

This article compares with other methods found in the literature, and the literature used for comparison mainly includes two parts, namely, literature related to relay motion

control based on different channel models and literature related to relay motion control based on different channel-prediction methods. First, this article compares the literature based on different channel models, namely, literature 26 and literature 27. The channel model used in literature 26 only considers the distance factor, without considering the transmission power and channel attenuation, while the channel model used in literature 27 simultaneously considers the effects of distance, transmission power, and channel attenuation. On the basis of considering these three influencing factors, this article further considers the influence of building height and distribution density in different urban areas on signal propagation. Therefore, the methods of literature 26 and 27 are selected for comparison. The difference in the relay implementation effect will be more obvious, thus reflecting the difference in the effects achieved by the relay motion-control methods based on different channel models. Then, this article compares relevant literature based on different channel-prediction methods, namely, literature 35 and literature 21, because they consider relay application scenarios similar to this article, namely, UAV relay in complex urban environments. At the same time, since different channel-prediction methods have requirements for their own application scenarios and may not be applicable to other relay scenarios, literature 35 and literature 21 are selected.

5.1. Simulation Parameters Setting

In the simulation, the motion of the UGV follows the smooth turning model [23]. The UAV is a fixed-wing aircraft and has kinematic constraints. The UAV can obtain the position information of the UGV but cannot obtain the instantaneous velocity (including size and direction) information of the UGV, nor can it obtain the future position information of the UGV. However, the Kalman Filter algorithm described in Section 2.4 is used for estimation. In the last experiment, the UAV does not know the wireless channel parameters in advance, but estimates them based on the channel-estimation model based on Gaussian process learning given in Section 2.2.

The environmental area is divided into four types [25], and the channel model parameters corresponding to each type of area are shown in Table 1, with the coverage range shown in Table 2.

Table 1. Wireless channel parameters for various types of areas.

Channel Parameter	Suburban	Urban	DenseUrban	HighRiseUrban
α	0.1	0.3	0.5	0.5
β	750	500	300	300
γ	8	5	20	50
a	5.0188	9.6101	11.9480	27.1562
b	0.3511	0.1592	0.1359	0.1228
$\eta_{\mathrm{LoS}}(\mathrm{dB})$	0.1	1.0	1.6	2.3
$\eta_{\mathrm{NLoS}}(\mathrm{dB})$	21	22	23	34

Table 2. Coverage of various types of areas.

Environmental Areas	Coverage Center		Coverage Radius (m)
	X(m)	Y(m)	
Suburban	6000	7000	9000
Urban	6490	4480	3600
DenseUrban	7000	3150	2000
HighRiseUrban	7340	2300	600

In order to examine the impact of the environments on channel characteristics and the performance of motion-control algorithms based on different models, comparative experiments are conducted, including two scenarios where the UAV supports point-to-point communication and multi-node communication. The comparative algorithms include

an algorithm based on a simple distance channel model (DCM) [27], an algorithm based on a statistical distribution probability channel model (SDPCM) [28], and an algorithm based on an average gain probability channel model (AGPCM). In addition, in the final simulation under unknown channel parameters, the method proposed in this article is also compared with the least square estimation (LSE)-based algorithm [35] and the neural network estimation (NNE)-based algorithm [21].

5.2. Stationary Nodes

Using the UAV to support stationary node communication is a simple and common scenario. In the first simulation, the point-to-point relay communication between two stationary UGVs is verified. The initial positions, transmission power, and channel attenuation factors of the ground nodes and the relay UAV are shown in Table 3. It is assumed that the channel parameters of the UGVs are known to the UAV in advance, and the signal frequency is $f_c = 2$ GHz. The speed of the UAV is 40 m/s, the desired flying radius is 200 m, and the maximum roll angle is 40°. The simulation time is 300 s.

Table 3. Parameters for the UGVs and the relay UAV (stationary nodes).

Item	X Coordinate	Y Coordinate	Transmission Power	Attenuation Factor
UGV 1	370 m	2348 m	200 mW	2.2
UGV 2	7701 m	2194 m	100 mW	2.4
Relay UAV	3210 m	6626 m	\	\

Figure 4 shows the simulation results, where circles of different colors represent the boundaries of different types of environmental areas, and curves of different colors represent the UAV relay flight trajectories obtained using different methods; the corresponding communication performance change curves are shown in Figure 5.

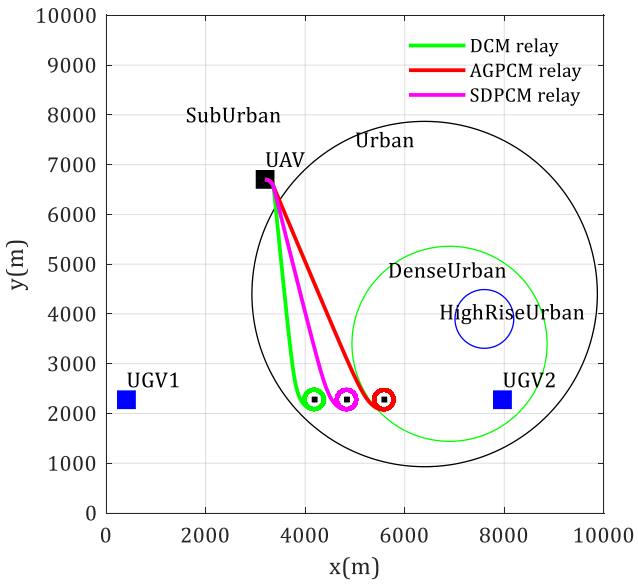

Figure 4. Flight trajectories of the UAV that supports communication for two stationary UGVs.

The simulation results show that the DCM (distance channel model)-based motion control algorithm drives the UAV to fly around the center of the two UGVs, while the SDPCM (statistical distribution probability channel model)-based motion control algorithm drives the UAV to fly closer to the UGV 2 with smaller transmission power, and the AGPCM(average gain probability channel model)-based motion control algorithm simultaneously takes into account that the UGV 2 has a smaller transmission power and is located in the HighRiseUrban area, where the signal attenuation rate is much greater than that of

the Suburban area where the UGV 1 is located. Therefore, it adjusts the UAV to fly closer to the UGV 2. This is also the reason why the initial positions of UGV 1 and UGV 2 are selected in Suburban and DenseUrban, respectively, when selecting simulation parameters. This is because only by making such a selection can the impact of the environment on the channel characteristics be reflected, and then the difference in the implementation effects of motion-control methods based on different channel models can be shown.

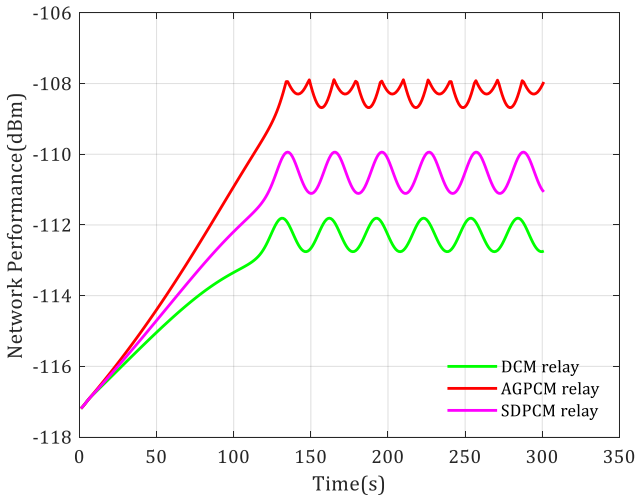

Figure 5. Changes in communication performance when the UAV supports communication for two stationary UGVs.

Obviously, this result is more in line with the actual situation, which verifies that it is valuable to consider the influence of environmental characteristics on the channel when designing the relay UAV motion-control algorithm. It also shows that it is more reasonable to measure the communication performance of the network based on AGPCM. Figure 5 verifies that the communication performance brought by AGPCM-based motion control method is better than the other two methods.

The second simulation experiment is to verify the use of the UAV to support communication for multiple stationary UGVs. There are 5 stationary UGVs in the task area, with positions of (1500, 1700), (3500, 8000), (2400, 5600), (8000, 4000) and (6000, 3000), respectively, in meters, as illustrated by the blue squares in Figure 6. The transmission power is randomly generated between 100∼200 mW. The initial position of the relay UAV is (3195, 6704), in meters, as shown by the black square in Figure 6. It is also assumed that the UAV has known the channel parameters, and other parameters are set the same as the previous experiment. The simulation results are shown in Figure 6 and Figure 7, respectively. The former gives the flight trajectories of the UAV based on different channel models, and the latter gives the corresponding communication performance change curves.

From Figure 6, it can be observed that the UGV 4 is located in the HighRiseUrban area. Due to the high-density and high-altitude buildings, the wireless information transmission in this area has a low probability of LoS occurrence, resulting in extremely poor communication conditions for the UGVs in this area. By comparing the three different colored relay paths, it can be found that the AGPCM-based motion control algorithm can drive the UAV to a better target position than the DCM-based and SDPCM-based motion control algorithms. In addition, the communication performance change curves in Figure 7 also verify this point because the communication performance curve obtained by the AGPCM-based algorithm is always at the highest position among the three, with the best communication performance, the best relay communication effect, and stable performance.

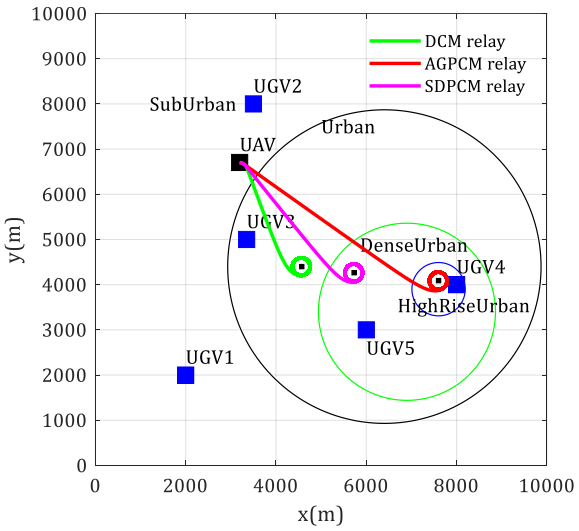

Figure 6. Flight trajectories of the UAV that supports communication for multiple stationary UGVs.

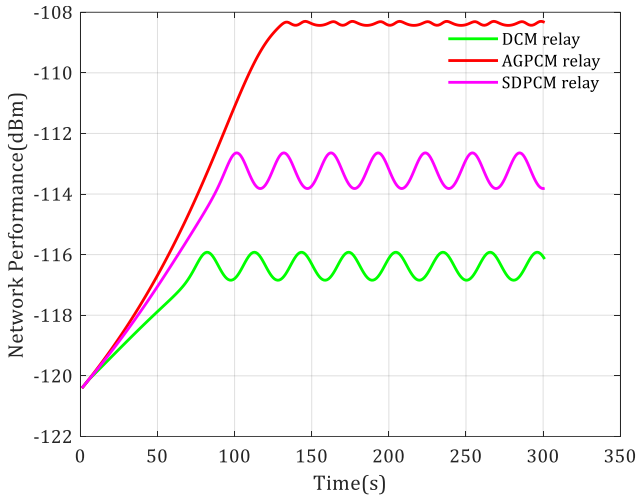

Figure 7. Changes in communication performance when the UAV supports communication for multiple stationary UGVs.

5.3. Moving Nodes

This section discusses the scenario of using relay UAV to support communication for moving UGVs with known parameters.

In the third simulation, there are two moving UGVs, namely, relay for point-to-point communication. The transmission power of the two UGVs is 100 mW and 200 mW, respectively. The motion trajectory is randomly given according to the smooth turning model, with a speed of 10 m/s. The blue square points in Figure 8 give their initial positions, and the connected blue solid lines are the motion trajectories of the UGVs. The UAV flies at a speed of 40 m/s, with a maximum roll angle of 40° and a desired flying radius of 200 m, and its initial position is shown by the black square points in Figure 8. The simulation time is 720 s.

Figure 8 shows the flight trajectories of the UAV based on different channel models, and the corresponding communication performance changes are shown in Figure 9. In order to reflect the impact of the environment on channel characteristics, especially the high altitude and high-density buildings in the HighRiseUrban environment, which lead to extremely poor communication conditions and sudden changes in network performance, we specifically let the trajectory of UGV1 pass through the HighRiseUrban area during the simulation. From Figure 9, it can be observed that there is a sudden change in the

communication performance, which is due to the UGV 1 moving to the HighRiseUrban area, resulting in extremely poor channel quality. The results of the three algorithms responding to this sudden change show that the AGPCM-based motion-control algorithm has the best performance, and in other non-sudden situations, the results of this algorithm can also provide the same or better performance as other algorithms.

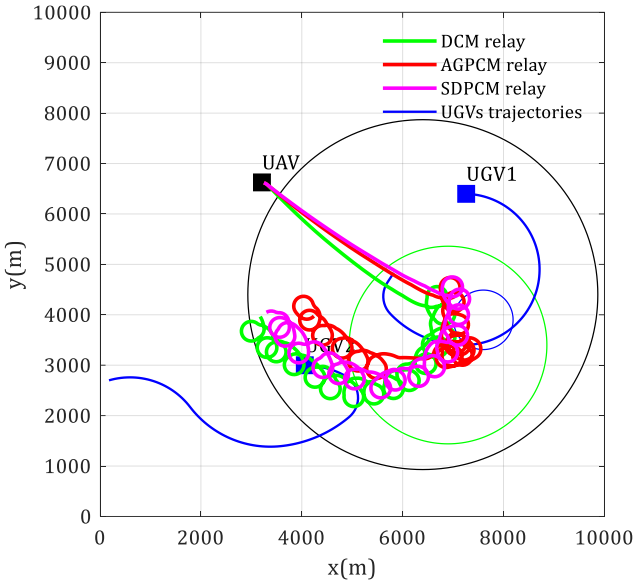

Figure 8. Flight trajectories of the UAV that supports point-to-point communication for two moving UGVs.

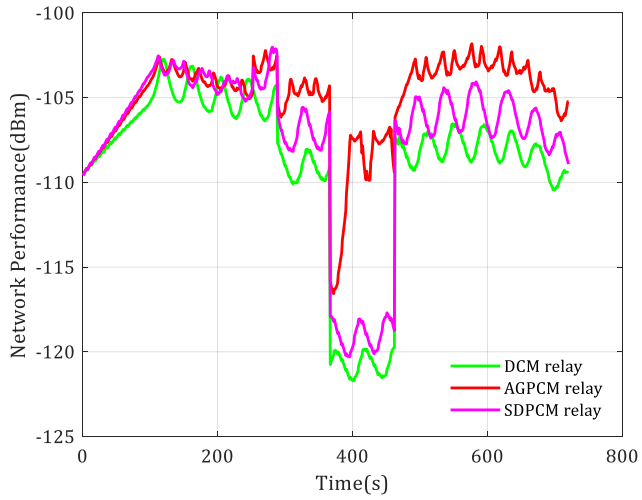

Figure 9. Changes in communication performance when the UAV supports point-to-point communication for two moving UGVs.

The fourth simulation is used to verify the scenario of using UAV to support communication for multiple moving UGVs. There are 6 UGVs, and the blue square points in Figure 10 represent their starting position. The blue solid line starting from these points represent the motion trajectories of the unmanned vehicles, which are randomly generated under the smooth turning model [21]. The motion speed is 10 m/s, and the transmission power is randomly generated between 100∼250 mW. Other parameters are the same as the third simulation. The simulation results are shown in Figures 10 and 11.

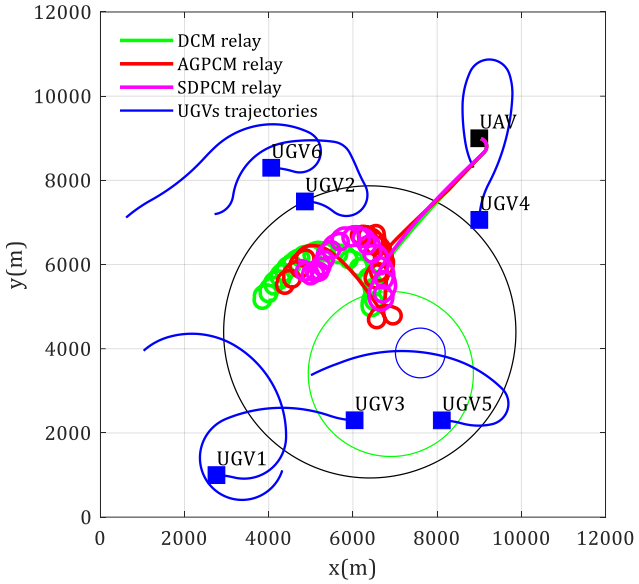

Figure 10. Flight trajectories of the UAV that supports multi-node communication for multiple moving UGVs.

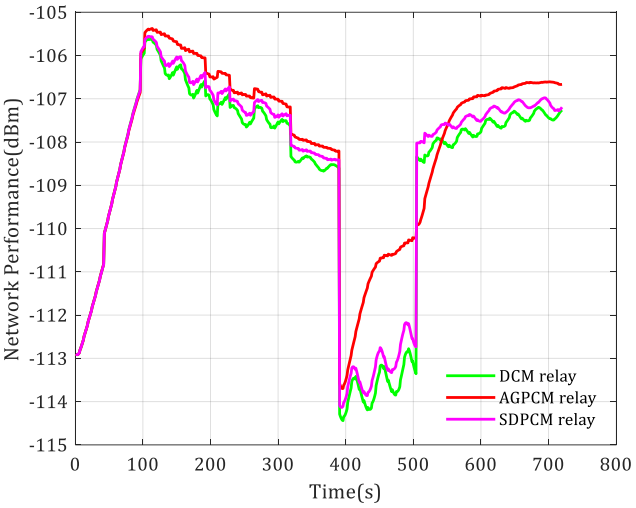

Figure 11. Changes in communication performance when the UAV supports multi-node communication for multiple moving UGVs.

As can be seen from Figure 11, there is also a sudden change in communication performance. This is because the UGV 5 entered the HighRiseUrban area within the time period of 391~504 s, causing the channel quality to become very poor. There are six unmanned ground vehicles, and the motion control algorithm based on AGPCM achieves the best relay communication performance, especially in the case of sudden changes in the communication environment.

The results of simulations 3 and 4 show that the online autonomous motion-control algorithm for the relay UAV proposed in this paper can effectively support the communication for moving UGVs and achieve good communication performance. In addition, considering the impact of the environments on the channel characteristics in the algorithm can bring better communication performance.

5.4. Moving Nodes with Unknown Channel Parameters

This section further discusses the simulation of adaptive online autonomous motion control of the relay UAV supporting communication of moving UGVs under unknown

channels. This scenario is also common and most complex in practical applications, requiring the UAV to estimate the wireless channel parameters and the power distribution in the environmental area based on limited sampling. The parameter settings are the same as those in Section 5.3, with the difference being that in this simulation, the channel parameters between the UAV and the UGVs are unknown in advance but are estimated by the Gaussian process learning algorithm in Section 2.2.

Figures 12 and 13 show the UAV flight trajectories and communication performance change curves, respectively. In Figures 12 and 13, by comparing the red curve and the cyan curve, we can see the performance gap between the proposed method in known channels and unknown channels. By comparing the cyan curve and the black curve, we can see the difference in the implementation effects of the proposed GP-based channel estimation method and the LSE(least square estimation)-based channel estimation method. By comparing the green curve and the pink curve, we can see the difference in the implementation effects of the NNE(neural network estimation)-based channel estimation method and the GP-based channel estimation method proposed in this paper. By comparing the cyan curve and the green curve, we can see the difference in the implementation effects of the methods based on different channel models. From the two figures, it can be seen that (1) although the performance of the UAV relay motion-control algorithm under unknown channel parameters proposed in this paper has not reached the theoretical optimal value under known channels, it has already approached the latter; (2) the air-to-ground channel parameter-estimation algorithm based on Gaussian process learning and AGPCM proposed in this paper can effectively estimate the air-to-ground channel parameters; and (3) the results based on the AGPCM algorithm are better than those based on the SDPCM algorithm, especially when the environmental characteristics of the UGVs change. (4) The communication performance obtained by the channel estimation algorithm based on Gaussian process learning is superior to that of the channel estimation algorithms based on LSE and NNE.

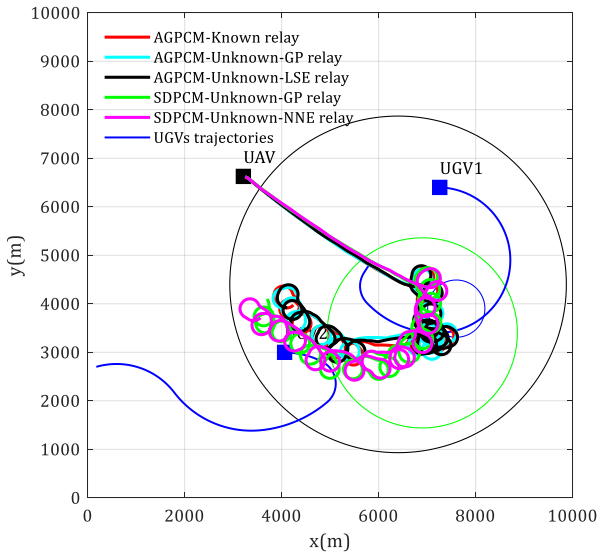

Figure 12. Flight trajectories of the UAV that supports point-to-point communication for two moving UGVs with unknown channel parameters.

Similarly, simulation is conducted on relay for multiple moving UGVs with unknown channel parameters, and the results are shown in Figures 14 and 15. By comparing the flight trajectories in Figure 14 and the communication performance changes in Figure 15, the same conclusion can be drawn.

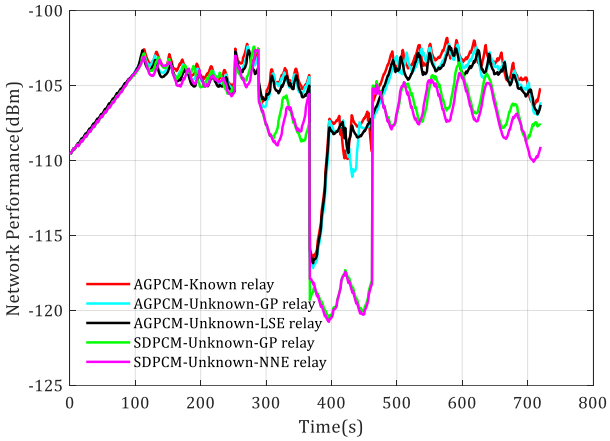

Figure 13. Changes in communication performance when the UAV supports point-to-point communication for two moving UGVs with unknown channel parameters.

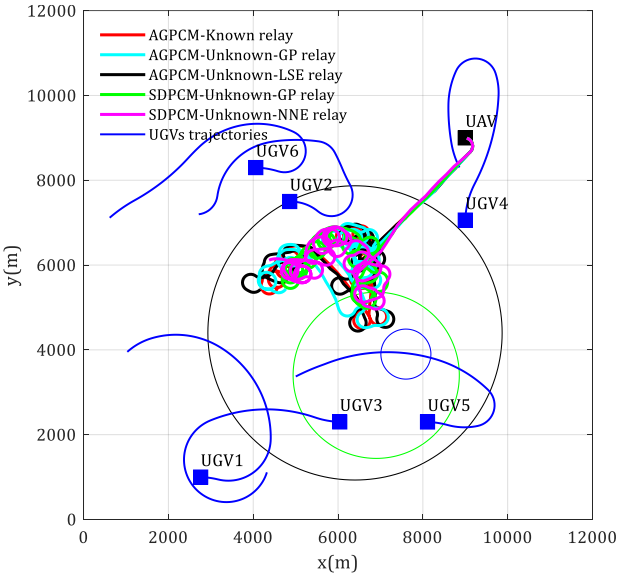

Figure 14. Flight trajectories of the UAV that supports multi-node communication for multiple moving UGVs with unknown channel parameters.

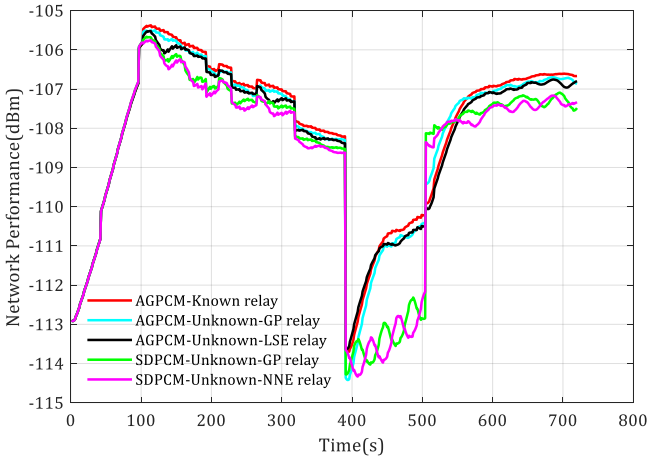

Figure 15. Changes in communication performance when the UAV supports multi-node communication for multiple moving UGVs with unknown channel parameters.

6. Conclusions

This article solves the problem of using the UAV as an aerial node to support multi-UGV communication in urban environments by jointly considering unknown radio frequency (RF) channel parameters, unknown multi-agent mobility, the impact of the environments on channel characteristics, and the unavailable angle of arrival (AoA) information of the received signals. The problem mainly includes two aspects: channel estimation and optimal relay position search. For the former, a Gaussian process (GP) learning method is proposed to estimate the unknown channel between the UAV and the UGV. It only needs to collect RSS data online, and the prediction effect of this method is better than that of the LSE and CE algorithms. For the latter, a line search algorithm for point-to-point communication and a gradient-based algorithm for multi-node communication are proposed, respectively. Both algorithms only need one-dimensional search, and the convergence conditions and stability proofs of the algorithms are given. Finally, the comparative experimental results under different conditions show that the online autonomous motion-control method of the relay UAV proposed in this article can effectively drive the UAV to reach or track changes in the optimal relay positions, and it is demonstrated that considering the impact of the environments on channel characteristics can bring better relay communication performance.

Future research directions could be (1) extending single-UAV relay to multi-UAV relay; (2) considering the motion control of relay UAVs with obstacle and threat avoidance; (3) considering the impact of UAV height on relay performance, that is, the motion control of relay UAVs in a three-dimensional environment; and (4) considering the optimization of other communication indicators, such as latency, bit error rate, etc.

Author Contributions: Conceptualization, C.T. and B.L.; methodology, C.T.; software, C.T.; validation, C.T. and B.L.; formal analysis, C.T. and B.L.; investigation, C.T.; resources, C.T.; data curation, C.T.; writing—original draft preparation, C.T.; writing—review and editing, C.T. and B.L.; visualization, C.T.; supervision, C.T.; project administration, C.T. and B.L.; funding acquisition, C.T. All authors have read and agreed to the published version of the manuscript.

Funding: This research received no external funding.

Data Availability Statement: Dataset available upon request from the authors.

Conflicts of Interest: The authors declare no conflict of interest.

References

1. Guan, Y.; Zou, S.; Peng, H.; Ni, W.; Sun, Y.; Gao, H. Cooperative UAV Trajectory Design for Disaster Area Emergency Communications: A Multi-Agent PPO Method. *IEEE Internet Things J.* **2023**, *56*, 2419–2430. [CrossRef]
2. Xu, L.; Cao, X.; Du, W.; Li, Y. Cooperative path planning optimization for multiple UAVs with communication constraints. *Knowl. Based Syst.* **2023**, *26*, 150–164. [CrossRef]
3. Nasim, I.; Ibrahim, A.S. Relay Placement for Maximum Flow Rate via Learning and Optimization over Riemannian Manifolds. *IEEE Trans. Mach. Learn. Commun. Netw.* **2023**, *15*, 216–229. [CrossRef]
4. Javaid, S.; Saeed, N.; Qadir, Z.; Fahim, H.; He, B.; Song, H.; Bilal, M. Communication and Control in Collaborative UAVs: Recent Advances and Future Trends. *IEEE Trans. Intell. Transp. Syst.* **2023**, *24*, 5719–5739. [CrossRef]
5. Mozaffari, M.; Saad, W.; Bennis, M.; Debbah, M. Mobile unmanned aerial vehicles (UAVs) for energy-efficient Internet of Things communications. *IEEE Trans. Wirel. Commun.* **2017**, *16*, 7574–7589. [CrossRef]
6. Tang, Q.; Yu, Z.; Jin, C.; Wang, J.; Liao, Z.; Luo, Y. Completed tasks number maximization in UAV-assisted mobile relay communication system. *Comput. Commun.* **2022**, *187*, 20–34. [CrossRef]
7. Dixon, C.; Frew, E.W. Optimizing cascaded chains of unmanned aircraft acting as communication relays. *IEEE J. Sel. Areas Commun.* **2012**, *30*, 883–898. [CrossRef]
8. Bor-Yaliniz, R.I.; El-Keyi, A.; Yanikomeroglu, H. Efficient 3-D placement of an aerial base station in next generation cellular networks. In Proceedings of the 2016 IEEE International Conference on Communications (ICC), Kuala Lumpur, Malaysia, 22–27 May 2016; pp. 1–5.
9. Choi, D.H.; Kim, S.H.; Sung, D.K. Energy-efficient maneuvering and communication of a single UAV-based relay. *IEEE Trans. Aerosp. Electron. Syst.* **2014**, *50*, 2320–2327. [CrossRef]
10. Huang, X.; Fu, X. Fresh data collection for UAV-assisted IoT based on aerial collaborative relay. *IEEE Sens. J.* **2023**, *23*, 8810–8825. [CrossRef]

11. Kim, S.; Oh, H.; Suk, J.; Tsourdos, A. Coordinated trajectory planning for efficient communication relay using multiple UAVs. *Control Eng. Pract.* **2015**, *29*, 42–49. [CrossRef]
12. Lun, Y.; Yao, P.; Wang, Y. Trajectory optimization of SUAV for marine vessels communication relay mission. *IEEE Syst. J.* **2020**, *14*, 5014–5024. [CrossRef]
13. Ouyang, J.; Zhuang, Y.; Lin, M.; Liu, J. Optimization of beamforming and path planning for UAV-assisted wireless relay networks. *Chin. J. Aeronaut.* **2014**, *27*, 313–320. [CrossRef]
14. Han, S.I. Survey on UAV deployment and trajectory in wireless communication networks: Applications and challenges. *Information* **2022**, *13*, 389. [CrossRef]
15. Chamseddine, A.; Akhrif, O.; Charland-Arcand, G.; Gagnon, F.; Couillard, D. Communication relay for multiground units with unmanned aerial vehicle using only signal strength and angle of arrival. *IEEE Trans. Control Syst. Technol.* **2017**, *25*, 286–293. [CrossRef]
16. Zhan, P.; Yu, K.; Swindlehurst, A.L. Wireless relay communications with unmanned aerial vehicles: Performance and optimization. *IEEE Trans. Aerosp. Electron. Syst.* **2011**, *47*, 2068–2085. [CrossRef]
17. Oh, H.; Shin, H.S.; Kim, S.; Chen, W.H. Communication-aware trajectory planning for unmanned aerial vehicles in urban environments. *J. Guid. Control. Dyn.* **2018**, *41*, 2271–2282. [CrossRef]
18. Yin, D.; Yang, X.; Yu, H.; Chen, S.; Wang, C. An air-to-ground relay communication planning method for UAVs swarm applications. *IEEE Trans. Intell. Veh.* **2023**, *8*, 2983–2997. [CrossRef]
19. Wu, G.; Gao, X.; Fu, X.; Wan, K.F.; Di, R.H. Mobility control of unmanned aerial vehicle as communication relay in airborne multi-user systems. *Chin. J. Aeronaut.* **2019**, *32*, 1520–1529. [CrossRef]
20. Kim, J.; Ladosz, P.; Oh, H. Optimal communication relay positioning in mobile multi-node networks. *Robot. Auton. Syst.* **2020**, *129*, 103517. [CrossRef]
21. Ladosz, P.; Oh, H.; Zheng, G.; Chen, W.H. A hybrid approach of learning and model-based channel prediction for communication relay UAVs in dynamic urban environments. *IEEE Robot. Autom. Lett.* **2019**, *4*, 2370–2377. [CrossRef]
22. Wu, J.; Wang, H.; Li, N.; Yao, P.; Huang, Y.; Su, Z.; Yu, Y. Distributed trajectory optimization for multiple solar-powered UAVs target tracking in urban environment by Adaptive Grasshopper Optimization Algorithm. *Aerosp. Sci. Technol.* **2017**, *70*, 497–510. [CrossRef]
23. Wan, Y.; Namuduri, K.; Zhou, Y.; He, D.; Fu, S. A smooth-turn mobility model for airborne networks. *IEEE Trans. Veh. Technol.* **2013**, *62*, 3359–3370. [CrossRef]
24. Rigatos, G.G. Distributed filtering over sensor networks for autonomous navigation of UAVs. *Intell. Serv. Robot.* **2012**, *5*, 179–198. [CrossRef]
25. Al-Hourani, A.; Kandeepan, S.; Lardner, S. Optimal LAP altitude for maximum coverage. *IEEE Wirel. Commun. Lett.* **2014**, *3*, 569–572. [CrossRef]
26. Khuwaja, A.A.; Chen, Y.; Zhao, N.; Alouini, M.S.; Dobbins, P. A survey of channel modeling for UAV communications. *IEEE Commun. Surv. Tutor.* **2018**, *20*, 2804–2821. [CrossRef]
27. Di, B.; Zhou, R.; Duan, H. Potential field based receding horizon motion planning for centrality-aware multiple UAV cooperative surveillance. *Aerosp. Sci. Technol.* **2015**, *46*, 386–397. [CrossRef]
28. Kopeikin, A.; Ponda, S.S.; Inalhan, G. Control of communication networks for teams of UAVs. In *Handbook of Unmanned Aerial Vehicles*; Springer: Dordrecht, The Netherlands, 2015; pp. 1619–1654.
29. Holis, J.; Pechac, P. Elevation dependent shadowing model for mobile communications via high altitude platforms in built-up areas. *IEEE Trans. Antennas Propag.* **2008**, *56*, 1078–1084. [CrossRef]
30. ITU. Propagation Data and Prediction Methods for the Design of Terrestrial Broadband Millimetric Radio Access Systems. 2003.
31. Liu, M.; Chowdhary, G.; Da Silva, B.C.; Liu, S.Y.; How, J.P. Gaussian processes for learning and control: A tutorial with examples. *IEEE Control Syst. Mag.* **2018**, *38*, 53–86. [CrossRef]
32. Noack, M.M.; Sethian, J.A. Advanced stationary and nonstationary kernel designs for domain-aware gaussian processes. *Commun. Appl. Math. Comput. Sci.* **2022**, *17*, 131–156. [CrossRef]
33. Carfang, A.J.; Wagle, N.; Frew, E.W. Improving data ferrying by iteratively learning the radio frequency environment. In Proceedings of the 2014 IEEE/RSJ International Conference on Intelligent Robots and Systems, Chicago, IL, USA, 14–18 September 2014; pp. 1182–1188.
34. Chamseddine, A.; Akhrif, O.; Gagnon, F.; Couillard, D. Communication relay for multi-ground units using unmanned aircraft. In Proceedings of the 14th International Conference on Control, Automation, Robotics and Vision (ICARCV), Phuket, Thailand, 13–15 November 2016; pp. 1–6.
35. Malmirchegini, M.; Mostofi, Y. On the spatial predictability of communication channels. *IEEE Trans. Wirel. Commun.* **2012**, *11*, 964–978. [CrossRef]